GSA **DR2015001** accompanies Scire, A., Biryol, C.B., Zandt, G., and Beck, S., 2015, Imaging the Nazca slab and surrounding mantle to 700 km depth beneath the central Andes (18°S to 28°S), *in* DeCelles, P.G., Ducea, M.N., Carrapa, B., and Kapp, P.A., eds., Geodynamics of a Cordilleran Orogenic System: The Central Andes of Argentina and Northern Chile: Geological Society of America Memoir 212, p. 23–41, doi:10.1130/2015.1212(02).

Imaging the Nazca slab and surrounding mantle to 700 km depth beneath the Central Andes (18° to 28°S)

Alissa Scire[1], C. Berk Biryol[1], George Zandt[1], and Susan Beck[1]

[1]*Department of Geosciences, University of Arizona, 1040 E. 4th Street, Tucson, AZ 85721*

SUPPLEMENTAL MATERIAL

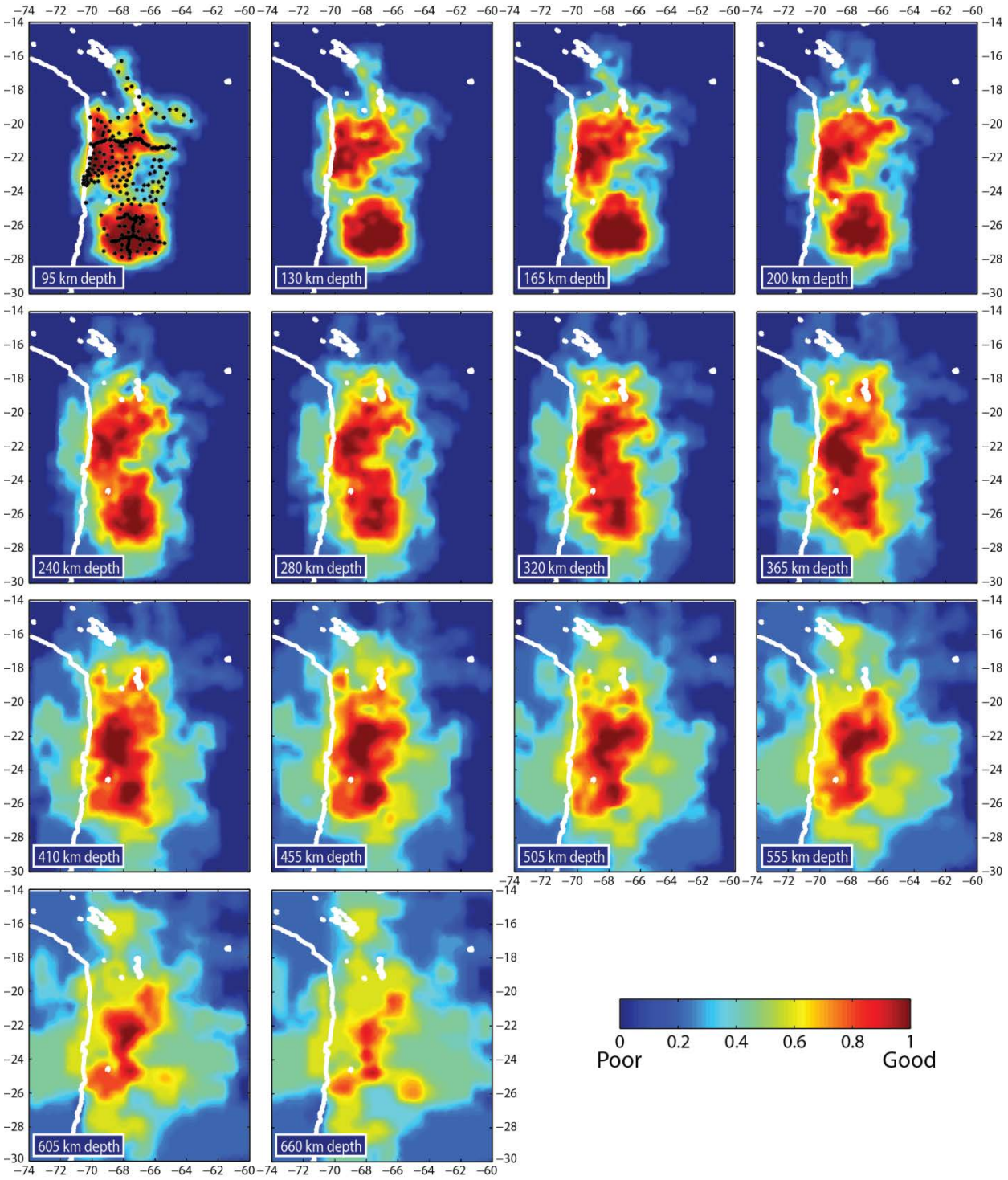

Figure S1. Normalized hit quality plots. Black stars on 95 km depth layer are station locations. Hit quality for a node is based on the number and azimuthal distribution of rays that sample that node. Good hit quality is indicated by red shading while poor hit quality is indicated by blue shading. Hit quality is strongly controlled by station distribution in uppermost depth slices with decreasing dependence on station distribution as depth increases.

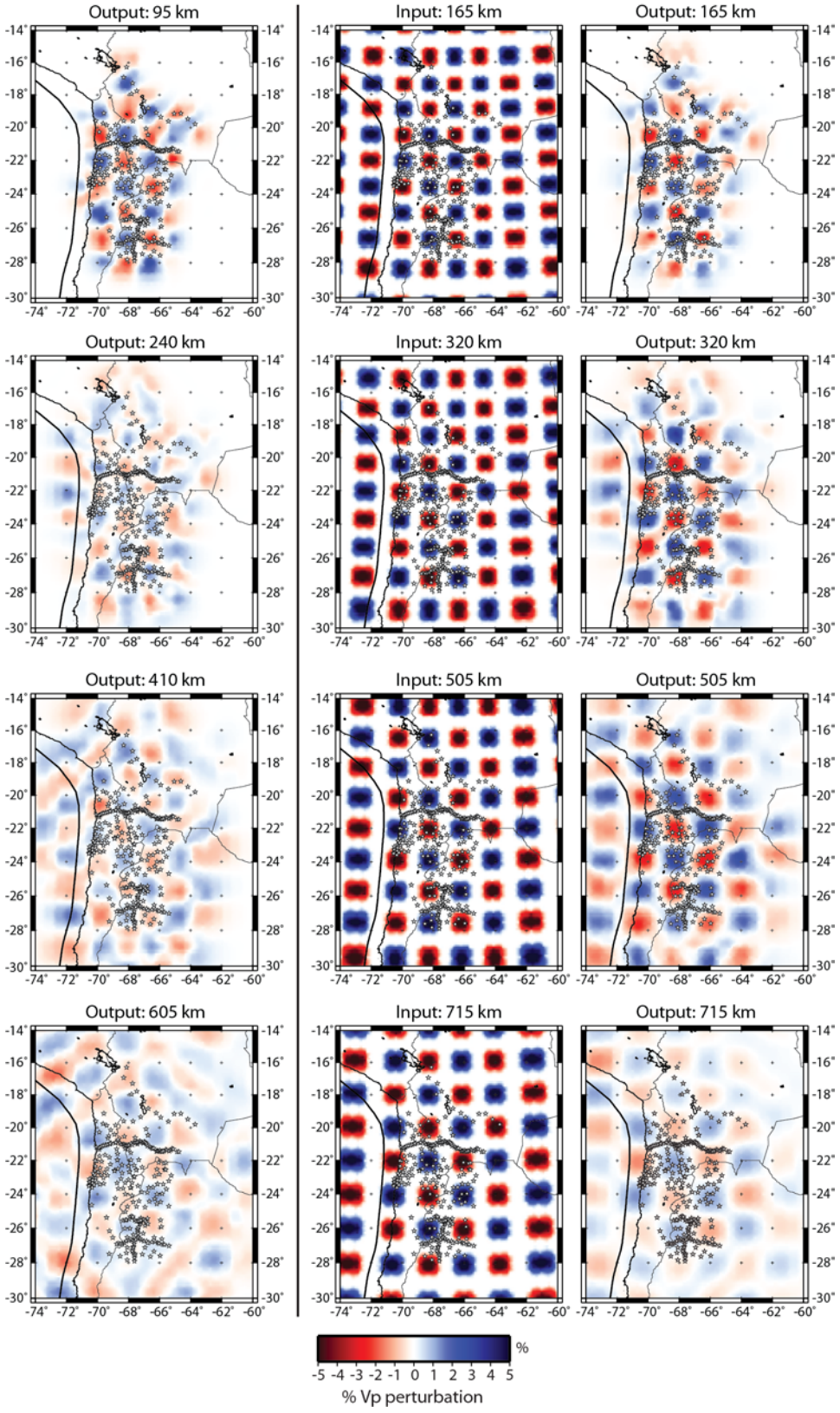
Output: 95 km
Input: 165 km
Output: 165 km
Output: 240 km
Input: 320 km
Output: 320 km
Output: 410 km
Input: 505 km
Output: 505 km
Output: 605 km
Input: 715 km
Output: 715 km
-14° -16° -18° -20° -22° -24° -26° -28° -30°
-74° -72° -70° -68° -66° -64° -62° -60°
-5 -4 -3 -2 -1 0 1 2 3 4 5
%
% Vp perturbation

Figure S2. Horizontal slices for checkerboard tests for every other model layer. Input for neutral layers (0% velocity deviation) is not shown. Output for neutral layers (95, 240, 410, 605 km depth) is shown in the left column. Resolution of velocity anomalies in neutral layers shown here indicates that vertical smearing is occurring. Checkerboard tests show that for shallower layers, resolution is controlled by station distribution as expected. Deeper model layers indicate that while the input amplitude cannot be completely resolved, lateral changes in anomalous velocity resolve with little horizontal smearing. Resolution is lost towards the edges of the model region.

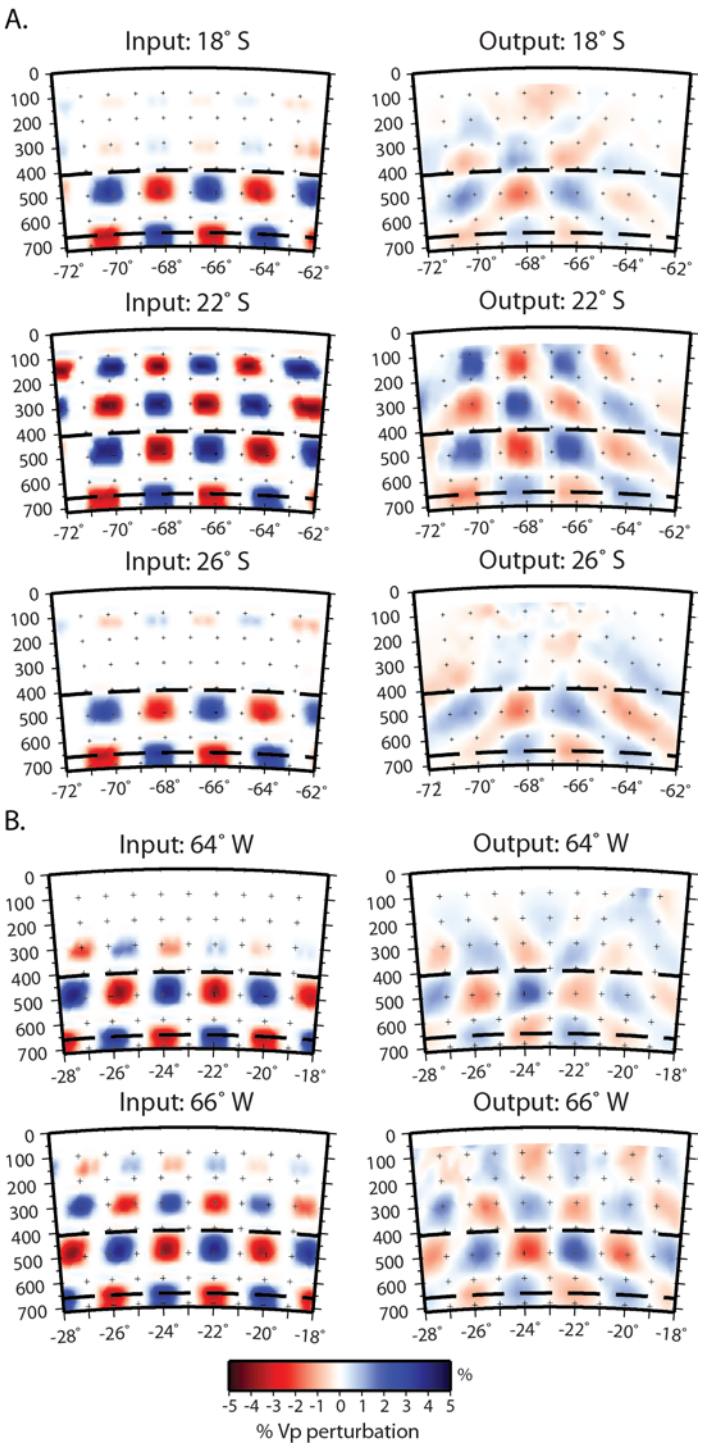

Figure S3. Cross sections through checkerboard tests. Irregular distribution of anomalies with depth in synthetic input (left) is due to the dilation of the node spacing with depth. A) E-W oriented cross sections through the synthetic input (left) and output (right) model. B) N-S oriented cross sections through the synthetic input (left) and output (right) model.

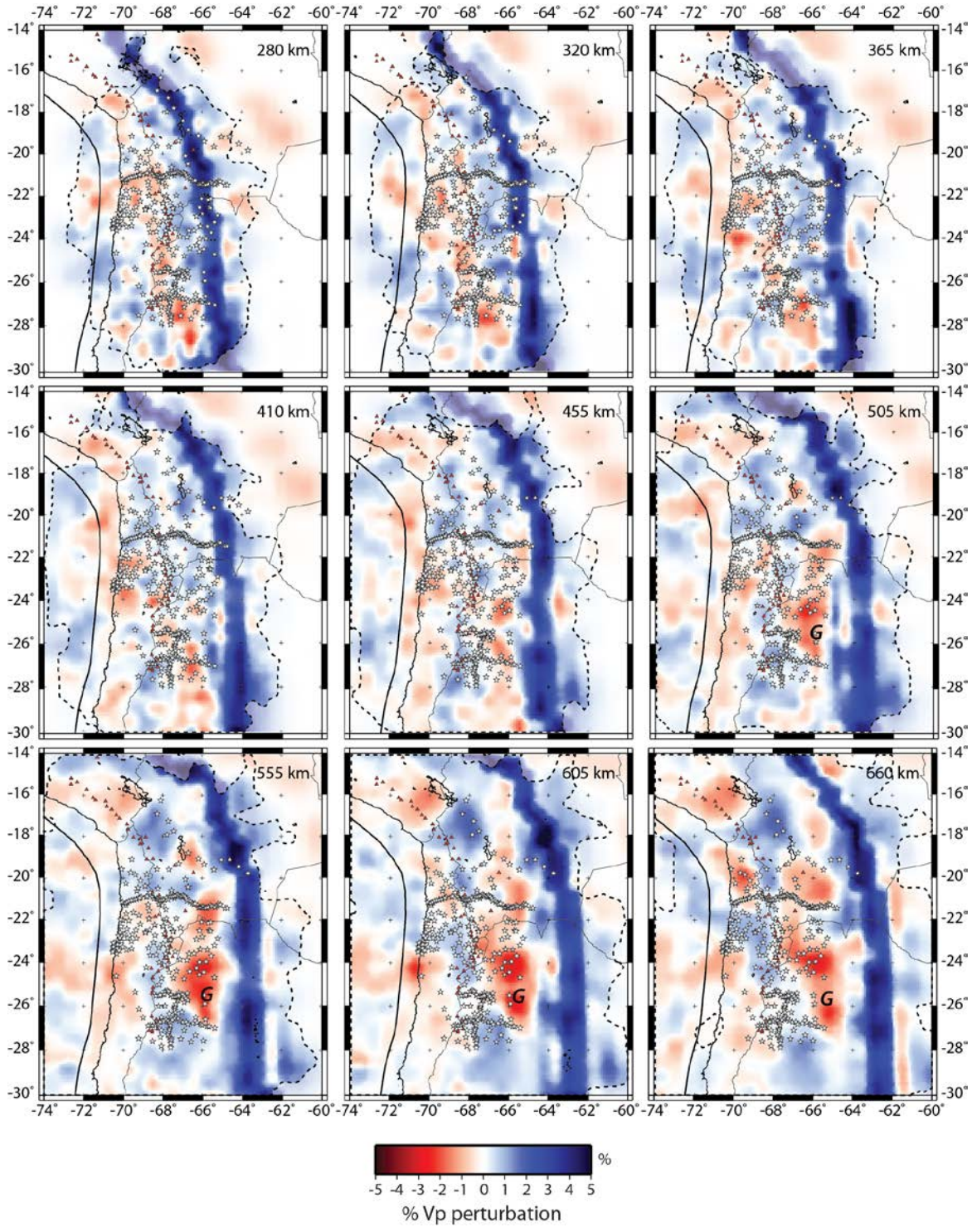

Figure S4. Horizontal depth slices from 280 to 660 km from the tomography model. Location of the Nazca slab is constrained using a priori information as discussed in the text. Dashed lines as in Figure 7. Stars mark locations of stations. Red triangles mark location of volcanoes. Black dots are earthquake locations from the EHB catalog (Engdahl et. al., 1998). Labeled anomaly G is discussed in the text.

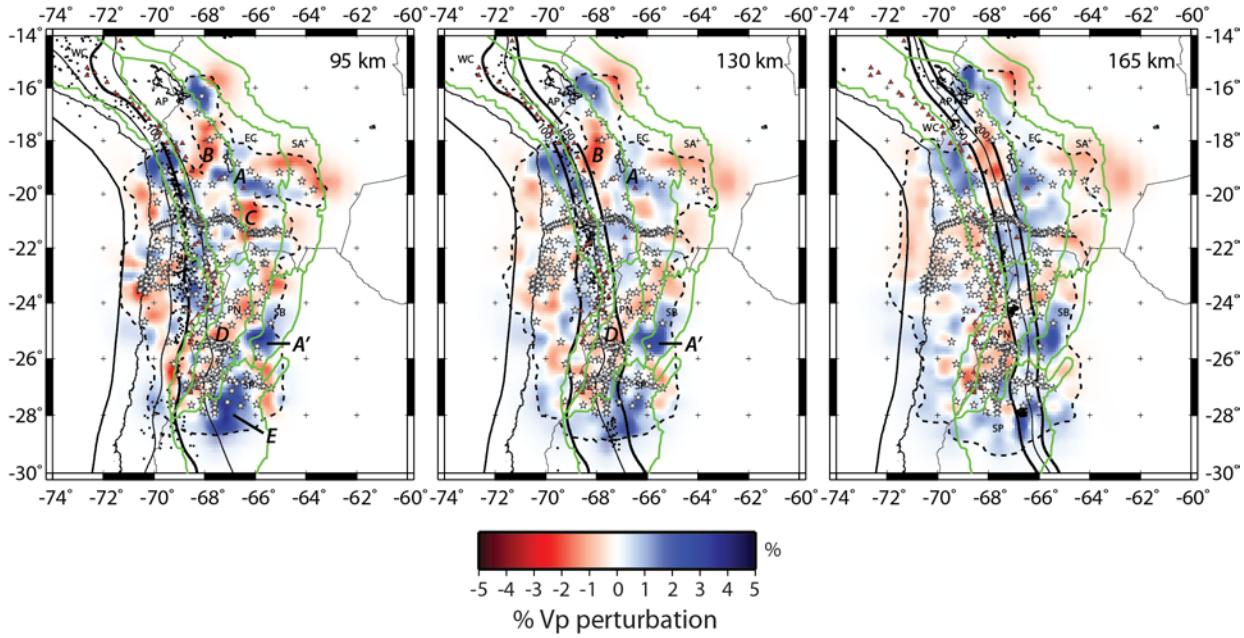

Figure S5. Horizontal depth slices for 95, 130, and 165 km from the tomography model without a priori constraints on the location of the subducting slab. Geomorphic provinces (green lines) same as in Figure 1a. Dashed lines as in Figure 7. Solid black lines are slab contours from Slab1.0 model (Hayes et. al., 2012). Labeled anomalies (A, A', B, C, D, and E) are discussed in the text.